Study on the Effect of Natural Aging and PAV Aging on Asphalt Binder Based on Rheology and Microstructural Composition

Fujin Hou , Yunding Zhu , Meng Guo * , Wenwu Zhang , Bolaxiake Hailati

Posted Date: 29 September 2025

doi: 10.20944/preprints202509.2463.v1

Keywords: natural aging; asphalt binder; aging behavior; discrepancies

Article

Study on the Effect of Natural Aging and PAV Aging on Asphalt Binder Based on Rheology and Microstructural Composition

Fujin Hou [1], Yunding Zhu [2,3], Meng Guo [2,3,*], Wenwu Zhang [1] and Bolaxiake Hailati [4]

[1] Shandong Hi-Speed Group Co., Ltd. Expressway Operation Center

[2] State Key Laboratory of Bridge Engineering Safety and Resilience, Beijing University of Technology, Beijing 100124, China

[3] The Key Laboratory of Urban Security and Disaster Engineering of Ministry of Education, Beijing University of Technology, Beijing 100124, China

[4] Tacheng Municipal Bureau of Housing and Urban-Rural Development

* Correspondence: gm@bjut.edu.cn

Abstract

Laboratory-simulated aging fails to fully replicate the complex aging behavior of asphalt binder under actual environmental conditions. This study aims to analyze the differences between natural aging and PAV aging of asphalt binder. In order to achieve the goal, indoor and natural environments were used to age the asphalt binder. The divergence in asphalt binder aging behavior was systematically investigated through encompassing low-temperature performance, chemical structure, elemental composition, molecular weight, and macroscopic and microscopic performance correlation analyses. Key findings include: The harsh environmental conditions in cold-arid region resulted in inferior low-temperature performance of naturally aged asphalt binder (12 months) compared to PAV-aged counterparts. Natural aging induced more significant asphalt binder's chemical structural changes than PAV aging, but exhibited less prominent oxidative reactions and macromolecular structure formation. Whether macroscopic or microscopic performance, hot oxygen was the main reason for the natural aging behavior of asphalt binder. The influence of other factors on the aging behavior of asphalt binder was not significant. The forced aging of PAV aging affected the cross-scale behaviors between oxygen content, molecular weight, and low-temperature performance in asphalt binder. This diminished the influence of oxygen content and molecular weight on the degradation of low-temperature performance, resulting in discrepancies compared to natural aging.

Keywords: natural aging; asphalt binder; aging behavior; discrepancies

1. Introduction

Flexible pavement has been widely adopted in high-grade highways worldwide due to its advantages such as enhanced driving safety and reduced noise pollution. During prolonged service exposure, flexible pavement inevitably undergoes degradation caused by environmental factors including elevated temperatures, oxygen, and solar radiation. This progressive deterioration of macroscopic performance under sustained environmental exposure is defined as flexible pavement aging [1–5]. Extensive investigations have demonstrated that aging induces bitumen hardening and embrittlement, accompanied by significant reductions in viscoelastic performance and crack resistance, ultimately leading to premature deterioration of pavement durability [6–8].

Considering the prolonged aging process of asphalt during actual service, researchers have consistently sought to simulate field aging in laboratory settings to expedite sample acquisition. Conventional methods include the Thin Film Oven Test (TFOT) and Rolling Thin Film Oven Test

 doi:10.20944/preprints202509.2463.v1

(RTFOT) to simulate short-term aging during production, mixing, and paving stages, while the Pressurized Aging Vessel (PAV) method replicates long-term field aging through high-temperature and high-pressure conditions. In recent years, numerous studies have employed these laboratory-based accelerated aging protocols, establishing standardized procedures for asphalt aging research. However, significant discrepancies persist between the continuous high-temperature/pressure conditions of simulated aging and actual pavement aging mechanisms. Under high ambient temperatures, asphalt pavement surfaces exhibit significantly elevated temperatures compared to surrounding air. Guan et al. reported that in most Chinese cities, summer atmospheric temperatures ranging between 30-40°C typically result in pavement temperatures not exceeding 70°C [9]. This shows that there is a large thermal difference between field conditions and laboratory simulations, as standardized PAV aging protocols employ sustained 100°C exposure - representing a 30°C+ temperature differential from actual pavement thermal regimes. Furthermore, PAV aging fails to consider the dynamic temperature variations inherent in natural environments due to diurnal and seasonal cycles. More critically, this accelerated aging protocol, which focuses solely on elevated temperature and pressure conditions, neglects the synergistic effects of multiple environmental factors encountered during actual pavement service. In fact, as early as 1961, Traxler discovered that light could accelerate the aging of asphalt binder [10]. Liu et al. revealed that during the ultraviolet (UV)-induced aging process of asphalt binder, molecular excitation and chemical bond cleavage occur. Under these effects, unstable chemical bonds within asphalt reach an excited state or fracture, thereby becoming more prone to oxidation reactions [11]. Zhao et al. further investigated the role of water in asphalt binder aging, demonstrating that water exhibits a certain inhibitory effect on UV-induced asphalt aging [12]. Additionally, some researchers have explored the impacts of unique environmental factors on asphalt binder aging, such as acid rain and saline water [13–15]. It is evident that compared to PAV aging, the actual natural environmental aging factors are more complex.

While comparative assessment of PAV aging and natural aging can be conducted through macroscopic performance degradation, asphalt binder's inherent complexity as a complex organic compound comprising approximately 300-2,000 distinct chemical constituents renders the microstructural aging processes exceedingly intricate [16]. Recent advancements in microscale aging characterization methodologies have enabled researchers to systematically investigate the evolutionary behavior of asphalt binder's internal microstructural composition during aging processes. This provided a powerful means to reveal the deep reason of asphalt binder macroscopic performance decline. Nuclear Magnetic Resonance (NMR) spectroscopy has proven effective in identifying chemical structural change during aging, including substitution, isomerization, fragmentation, association, polymerization, condensation, and cyclization [17–19]. Experimental investigations by Zhang, Di et al. have revealed that aging generates substitution reactions at hydrogen sites on aromatic rings, accompanied by isomerization of specific hydrocarbon types [20–22]. The dehydrogenation process generates free radicals that exhibit high reactivity with atmospheric oxygen, forming peroxy radicals. These reactive species abstract hydrogen atoms from adjacent asphalt binder molecules, thereby leading to radical chain reactions that ultimately lead to the formation of oxygen-containing functional groups [23–25]. Through Fourier Transform Infrared Spectroscopy (FTIR), Liu et al. quantitatively identified two dominant oxygenated polar functionalities - carbonyl (C=O) and sulfoxide (S=O) groups - formed during aging [26,27]. This chemical evolution drives systematic polarity alterations in asphalt binder fractions: low-polarity aromatic fractions progressively convert to higher-polarity resins, which subsequently transform into asphaltenes. Such compositional redistribution destabilizes the colloidal equilibrium within asphalt binder. Elemental analysis provides direct empirical evidence for characterizing asphalt binder oxidative aging, with measurable increases in oxygen content being quantitatively verified during aging processes [28,29]. Molecular-scale investigations employing Gel Permeation Chromatography (GPC) have revealed that asphalt binder aging significantly increases both average molecular weight and molecular dispersity [30,31]. These molecular-level changes amplify intermolecular friction forces within the asphalt binder, constraining molecular mobility and ultimately leading to

 doi:10.20944/preprints202509.2463.v1

deterioration in macroscopic performance. It is evident that aging induces evolutionary changes in the asphalt binder's microscale structure, which consequently affects its macroscopic performance. To gain a comprehensive understanding of the differences between natural aging and PAV aging effects on asphalt binder, it is necessary to conduct investigations from three perspectives: microscopic scale, macroscopic scale, and cross-scale behaviors.

This study aims to clarify the differences between natural aging and PAV aging behaviors of asphalt binder. Four aging styles were implemented: short-term aging, PAV aging, 12-month natural thermo-oxidative aging, and 12-month all-weather aging. The effects of these protocols on asphalt binder's low-temperature performance degradation, chemical structure evolution, elemental composition variation, and molecular weight distribution were systematically analyzed. Furthermore, macroscopic and microscopic performance correlation analyses revealed critical discrepancies between PAV aging and natural aging behaviors. These findings provide a theoretical foundation for calibrating deviations between laboratory-simulated aging and natural aging behaviors of asphalt binder, and for achieving accurate simulation of natural aging through controlled laboratory-simulated aging. The technological roadmap for the paper is shown in Figure 1.

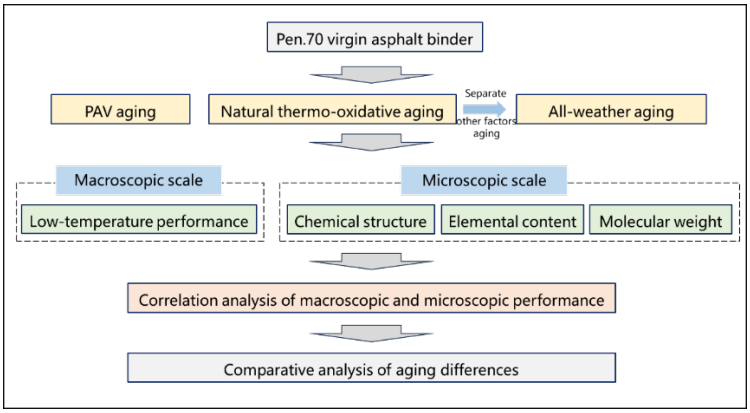

Figure 1. The technological roadmap.

2. Materials and Methods

2.1. Materials

The experiment employed Pen.90 virgin asphalt binder, with its fundamental technical indexes detailed in Table 1.

Table 1. Basic physical indexes of virgin asphalt binder.

Tests		Results	Limits	Standards
Penetration （25℃、100g、5s）/0.1mm		81.5	80~100	T0604-2011
Softening point （R&B）/℃		45	≥44	T0606-2011
Ductility （5cm/min、10℃）/cm		100	≥30	T0605-2011
Aging tests （163℃、5h）	The quality change/%	-0.13	≤±0.4	T0610-2011
	Penetration ratio/%	64	≥57	T0604-2011
	Residual ductility ratio/%	11	≥8	T0605-2011

 doi:10.20944/preprints202509.2463.v1

2.2. Test Methods

2.2.1. Laboratory-Simulated Aging Methods

As shown in Figure 2, the asphalt binder was placed in a thin-film oven for aging. The aging temperature was set to 163°C, and the asphalt binder was aged for 5 hours to obtain short-term aged asphalt binder. Subsequently, the short-term aged asphalt binder was transferred to a pressure aging vessel (PAV), where it underwent further aging at 100°C under 2.1 MPa pressure for 20 hours, resulting in long-term aged asphalt binder.

(**a**) (**b**)

Figure 2. Laboratory-simulated aging instruments for asphalt binder: (**a**) Thin-film oven; (**b**) Pressure aging vessel.

2.2.2. Natural Aging Methods

The natural aging of asphalt binder samples was conducted at the Field Scientific Observation and Research Station in the Cold-Arid Regions of Northwest China, located in Dunhuang City, Gansu Province. This region exhibits a dry climate with minimal rainfall, significant diurnal temperature fluctuations, and short, windy spring and autumn seasons. Frequent spring dust storms and intense ultraviolet radiation further define its environmental conditions. These complex climatic factors drive intricate aging behaviors in asphalt binder, severely undermining pavement durability.

To systematically compare PAV aging with natural aging, two distinct natural aging styles were applied to short-term thin-film oven-aged asphalt samples. All aging samples were mounted on racks 0.5 meters above ground level and subjected to a 12-month aging period under field conditions. The asphalt binder sample shown in Figure 3(a) was shielded by an opaque cover, restricting its exposure solely to temperature and oxygen while isolating it from light, water, dust, and other environmental factors. It was abbreviated as 12-O. This style designated as natural thermal-oxidative aging style. The asphalt binder sample depicted in Figure 3(b) was fully exposed to the natural environment, subjecting it to all environmental factors including light, moisture, and dust. This style, designated as all-weather aging style, enables systematic analysis of non-thermal-oxidative factors on asphalt binder aging. It was abbreviated as 12-A.

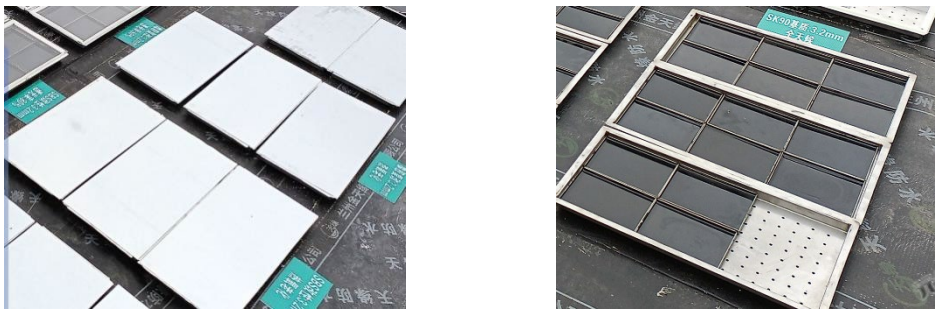

(**a**) (**b**)

 doi:10.20944/preprints202509.2463.v1

Figure 3. The natural aging style of asphalt binder: (**a**) Natural thermal-oxidative aging style; (**b**) All-weather aging style.

2.2.3. Test Methods for Low-Temperature Performance

The low-temperature performance of asphalt binder samples was evaluated using a dynamic shear rheometer (DHR-2) equipped with 4 mm aluminum parallel plates. Testing was conducted at three temperatures: -18°C, -12°C, and -6°C, with an angular frequency sweep ranging from 0.2 to 100 rad/s under controlled strain mode at 0.1%. The stiffness modulus (S) and creep rate (m) of the asphalt binder samples at these temperatures were calculated through frequency-temperature superposition analysis, thereby characterizing their low-temperature rheological behavior.

2.2.4. Test Methods for Chemical Structure

1. Chemical structure analysis

The experiments employed a nuclear magnetic resonance (NMR) spectrometer (ASCEND™ 400 [AVANCE HD III], Bruker Corporation, Germany) with a magnetic field strength of ≥9.39 T (400 MHz) and magnetic field drift ≤8 Hz/h. A 10 mg asphalt binder sample was dissolved in 0.5 mL of deuterated chloroform and subjected to NMR analysis. The acquired spectra were processed using TopSpin software to quantify assigned attributed hydrogen content, thereby characterizing the chemical structure of the asphalt binder.

2. Elemental content analysis

The experiments were performed using a Vario EL cube elemental analyzer (Elementar Analysensysteme GmbH, Germany) employing the micro-combustion method. Samples were encapsulated in tin containers and combusted at 1200°C to achieve complete decomposition. The resultant products were transported via helium carrier gas to the separation and detection unit, where they underwent adsorption-desorption processes for chromatographic separation.

3. Average molecular weight analysis

The experiments utilized a gel permeation chromatography (GPC) system (Waters 515-717-2410) equipped with a refractive index detector (Waters 2410) and a column set comprising three Waters Styragel columns (HT6E-HT5-HT3) connected in series. The column temperature was maintained at 35°C, and the elution flow rate was set to 1 mL/min. Calibration was performed using polystyrene (PS) standards with peak molecular weights ranging from 1.62-2.3 million, employing a 14-point calibration curve constructed from the PS standards. Asphalt samples were prepared at concentrations of 10–15 mg/mL in tetrahydrofuran (THF) as the mobile phase, with an elution flow rate of 1 mL/min. The number-average molecular weight (M_n), weight-average molecular weight (M_w), and polydispersity index (D) were calculated using Equations 1–3.

$$M_{\mathrm{n}} = \frac{\sum N_{\mathrm{i}} M_{\mathrm{i}}}{\sum N_{\mathrm{i}}} \tag{1}$$

$$M_{\mathrm{w}} = \frac{\sum N_{\mathrm{i}} M_{\mathrm{i}}^2}{\sum N_{\mathrm{i}} M_{\mathrm{i}}} \tag{2}$$

$$D = \frac{M_{\mathrm{w}}}{M_{\mathrm{n}}} \tag{3}$$

In the equations, M_{n} represents the number-average molecular weight, M_{w} represents the weight-average molecular weight, D represents the polydispersity index, and N_{i} represents the number of molecules with a molecular weight of M_{i}.

3. Results and Discussion

3.1. The Influence of Different Aging Styles on the Low-Temperature Performance of Asphalt Binder

As a temperature-sensitive material, asphalt binder exhibits viscoelastic properties that are significantly influenced by temperature. At low temperatures, its elastic characteristics become more pronounced, thereby increasing susceptibility to cracking [32]. The U.S. Strategic Highway Research

 doi:10.20944/preprints202509.2463.v1

Program (SHRP) introduced stiffness modulus (*S*) and creep rate (*m*) as key parameters for evaluating asphalt binder's low-temperature performance. The measured stiffness modulus and creep rate values of asphalt under different aging styles are presented in Figure 4.

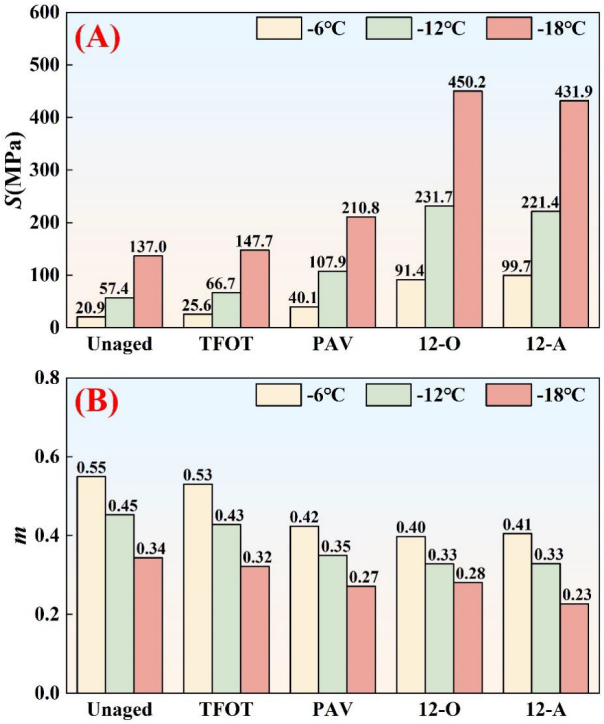

Figure 4. The stiffness modulus and creep rate of asphalt binder under different aging styles: (a) stiffness modulus; (b) creep rate.

The results demonstrated that asphalt binder exhibited distinct variations in stiffness modulus and creep rate under different aging styles, with stiffness modulus increasing and creep rate decreasing to varying degrees. These changes reflected deteriorated low-temperature flexibility and stress relaxation capacity, ultimately leading to impaired low-temperature performance. Compared to PAV aging, both 12-month natural thermal-oxidative aging and all-weather aging induced significantly greater alterations in stiffness modulus and creep rate. For instance, at -12°C, the stiffness modulus increased by 247.2% and 231.7% for natural thermal-oxidative aging and all-weather aging, respectively, relative to short-term aged asphalt binder. In contrast, PAV aging only caused a 61.6% increase in stiffness modulus under the same conditions, which was markedly lower than the impacts of natural aging. In cold-arid regions, extreme diurnal temperature fluctuations and prolonged daytime heat synergistically amplified aging rates, resulting in substantially accelerated degradation. Consequently, both natural aging modes produced far more severe low-temperature performance deterioration than PAV aging. Although PAV aging is widely considered equivalent to 3–10 years of natural aging [17], this equivalence depends critically on evaluation metrics, asphalt type, and climatic conditions. The complex aging conditions in cold-arid regions significantly accelerated the aging behavior of asphalt binder, thereby resulting in substantially inferior low-temperature performance of both naturally aged asphalt binder styles (thermal-oxidative and all-weather aging) compared to PAV-aged asphalt binders.

While asphalt binder in all-weather aging styles exhibited a higher stiffness modulus at -6°C compared to natural thermal-oxidative aging, it demonstrated lower stiffness modulus at -12°C and -18°C. The creep rate of them also exhibited varying magnitude relationships at different temperatures, leading to multiple types of changes in the low-temperature performance of all-weather aged asphalt compared to natural thermal-oxidative aged asphalt. But on the whole, this change was not significant, thus confirming that thermal-oxidative effects remain the dominant factor

 doi:10.20944/preprints202509.2463.v1

driving asphalt aging. In reality, all-weather aging introduced additional environmental influences—such as light, water, and dust—absent in natural thermal-oxidative aging. Similarly, ultraviolet (UV) radiation synergized with oxygen to induce photo-oxidative aging of asphalt binder. Water exerted dual opposing effects: it leached aromatic hydrocarbons from asphalt through a washing action [33]. while simultaneously forming surface water films that inhibited photo-oxidative aging of asphalt binder [34]. Concurrently, dust accumulation partially shielded asphalt binder from UV exposure, further inhibited the aging speed of asphalt binder. These complex interactions among light, water, and dust under natural conditions created complex aging-induced behaviors, ultimately manifesting as intricate low-temperature performance deterioration behaviors in asphalt binder.

3.2. The Influence of Different Aging Styles on the Chemical Structure of Asphalt

3.2.1. Chemical Structure Analysis

Nuclear magnetic resonance (NMR) technology has been widely applied in the chemical structural analysis of asphalt binder and organic compounds, enabling precise determination of hydrogen atoms' chemical environments in samples. Nuclear magnetic resonance (NMR) spectroscopy provides hydrogen-specific information including chemical shifts, coupling constants, and integral values, which correspond to absorption positions, peak splitting patterns, and absorption intensities, respectively. These three spectral features enable the deduction of hydrogen atom positions along carbon chains, thereby determining the chemical structure of the analyzed sample. H_A denotes hydrogen atoms directly bonded to aromatic carbons. H_α denotes hydrogen attached to α-carbons adjacent to aromatic rings. H_β denotes hydrogen on β-carbons of aromatic rings as well as CH_2 and CH groups outside β-positions. H_γ represents hydrogen on γ-carbons of aromatic rings and CH_3 groups outside γ-positions. Through peak integration within the respective spectral regions of H_A, H_α, H_β, and H_γ followed by normalization, the contents of these four attributed hydrogen types were quantitatively determined, as illustrated in Figure 5.

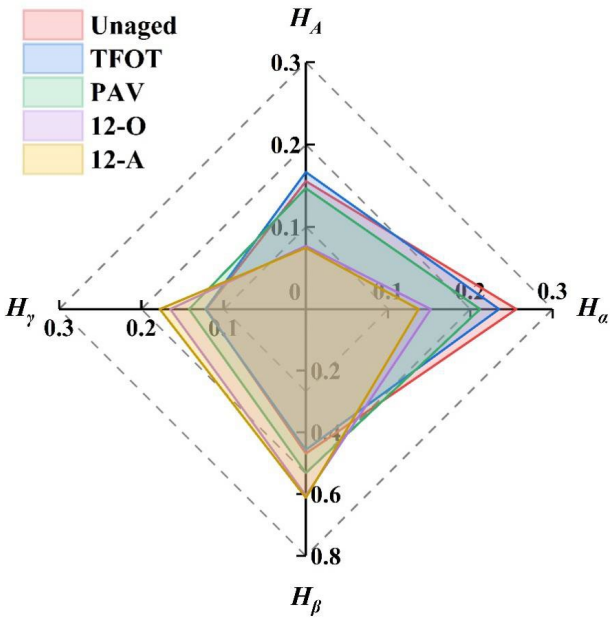

Figure 5. The attributed hydrogen content of asphalt binder under different aging styles.

The results demonstrated that after PAV aging, the H_A and H_α contents of asphalt binder exhibited certain reductions, indicating the occurrence of dehydrogenative condensation reactions on aromatic rings [20]. And the number of substituent groups on the aromatic rings of asphalt decreased. Furthermore, prolonged aging resulted in an increase in H_β and H_γ contents, indicating an accumulation of free chain structures within the asphalt binder. Following PAV aging, the H_A and H_α

 doi:10.20944/preprints202509.2463.v1

contents of asphalt binder decreased by 11.8% and 9.8%, respectively, compared to short-term aged asphalt binder, while H_{β} and H_{γ} contents increased by 16.4%. These results demonstrated that the chemical structure of asphalt undergoes more pronounced alterations under natural thermal-oxidative conditions, thereby significantly impacting its macroscopic performance. Following 12 months of all-weather aging, although minor increases or decreases in the four attributed hydrogen contents were observed compared to 12-month natural thermal-oxidative aging, these variations were not significant. This confirmed that thermal-oxidative aging is the main factor leading to the change of the chemical structure of asphalt binder.

3.2.2. Elemental Content Analysis

The aging process of asphalt binder is primarily driven by oxidation reactions. To further quantify the differences in oxidation reactions between natural aging styles and PAV aging, the oxygen content of asphalt binder under various aging styles were measured, as shown in Figure 6.

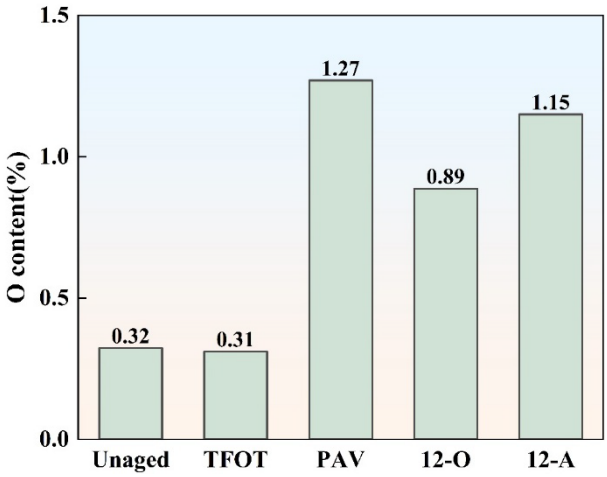

Figure 6. The content of *O* element in asphalt binder under different aging styles.

As shown in Figure 6, the oxygen content of asphalt binder significantly increased after long-term laboratory and natural aging. This rise was attributed to prolonged oxidation reactions that generate oxygen-containing groups within the asphalt binder. The asphalt binder subjected to PAV aging exhibited the highest oxygen content of 1.2%, demonstrating that more oxidation reactions occurred during the PAV aging process. After 12 months of natural thermal-oxidative aging, the oxygen content of asphalt binder was only 0.89%. Although the inclusion of light, water, and dust during 12-month all-weather aging increased the oxygen content compared to natural thermal-oxidative aging, it remained 9.4% lower than that of PAV-aged asphalt binder. This demonstrated that the high-temperature and high-pressure conditions of PAV aging significantly accelerate oxidation reactions in asphalt binder.

3.2.3. Molecular Weight Analysis

As a multicomponent composite material, asphalt binder consists of organic compounds with diverse molecular weights, resulting in a broad molecular weight distribution. During the aging process of asphalt binder, external environmental factors drive continuous chemical reactions among these compounds, generating new substances and altering the molecular weight profile of the asphalt. The molecular weight measurement results are shown in Figure 7.

 doi:10.20944/preprints202509.2463.v1

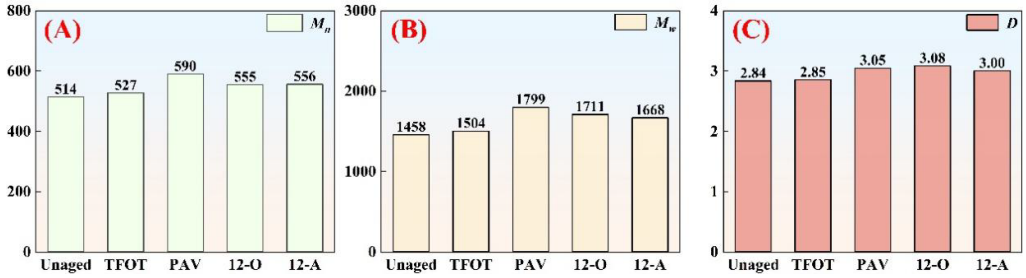

Figure 7. The molecular weight and distribution width of asphalt under different aging modes: (A) number-average molecular weight M_n; (B) weight-average molecular weight M_w; (C) polydispersity index D.

As shown in Figure 7, both the number-average molecular weight and weight-average molecular weight of asphalt increased under all aging styles, with PAV-aged asphalt binder exhibiting the highest molecular weights. This phenomenon correlates strongly with the intensified oxidation reactions of asphalt binder induced by PAV aging. The oxidation reactions of asphalt binder generated oxygen-containing polar functional groups. Electrostatic interactions between these polar groups further promoted the aggregation of smaller molecules into larger macromolecular structures through association and cross-linking. Consistent with elemental analysis results, although natural aging caused more severe low-temperature performance degradation compared to PAV aging, the magnitude of molecular weight increase in naturally aged asphalt binder was significantly lower than that of PAV-aged asphalt binder.

The polydispersity coefficient could characterize molecular weight distribution. Compared with short-term aging, PAV aging, natural thermal-oxidative aging, and all-weather aging increased asphalt binder's polydispersity coefficient by 6.8%, 8.1%, and 5.2% respectively, indicating enhanced molecular dispersion within asphalt binder. A higher polydispersity coefficient corresponds to reduced dispersibility of maltenes, which deteriorates asphalt binder's colloidal stability [35]. Thereby further deteriorated the low-temperature performance of asphalt binder.

 doi:10.20944/preprints202509.2463.v1

3.3. Correlation Analysis of Macroscopic and Microscopic Performance of Asphalt Binder Under Different Aging Styles

Previous studies demonstrate strong correlations between asphalt binder's macroscopic performance and microscopic composition, indicating that cross-scale behaviors exist where microstructural changes predict macroscopic performance variations [36–39]. Given PAV aging's forced aging characteristics, this forced aging process may modify asphalt binder's cross-scale behaviors of macro-micro performance compared to natural aging. Therefore, correlation analyses between asphalt binder's low-temperature performance and microscopic chemical composition were conducted across different aging styles. Low-temperature performance was quantified using the -12°C stiffness modulus, as detailed in Figure 8.

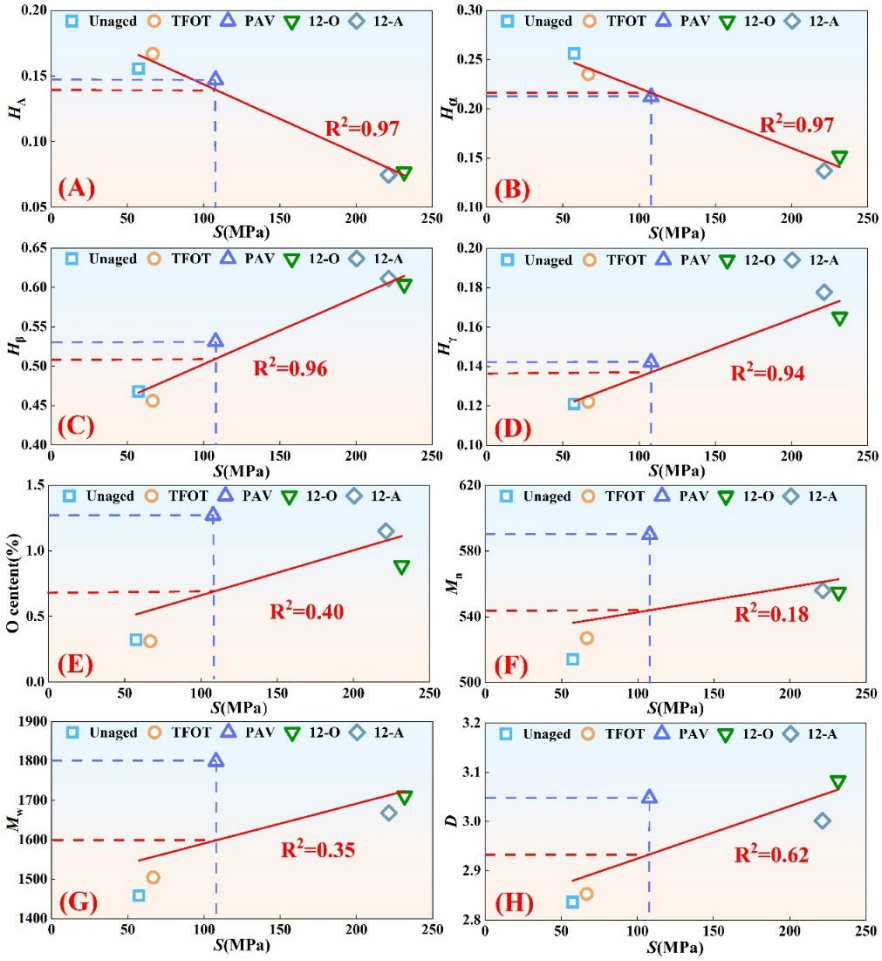

Figure 8. Correlation analysis of macroscopic and microscopic performance of asphalt binder under different aging styles: (A) Correlation between H_A and S; (B) Correlation between H_α and S; (C) Correlation between H_β and S; (D) Correlation between $H\gamma$ and S; (E) Correlation between O content and S; (F) Correlation between H_β and S; (G) Correlation between H_β and S.

As evidenced in Figure 8, although natural aging of asphalt binder involved exposure to light, water, dust, and other environmental factors, the inclusion of these factors did not significantly affect the cross-scale behaviors of its macro-micro performance. This phenomenon was likely attributable to the coupling effects of multiple factors, demonstrating that thermal-oxidative aging played a dominant role in governing the cross-scale behaviors of asphalt binder's macro-micro performance during natural aging.

The stiffness modulus of asphalt binder under different aging styles exhibited strong linear correlations with four attributed hydrogen (H_A, H_α, H_β, and H_γ), with all goodness-of-fit (R^2) values

 doi:10.20944/preprints202509.2463.v1

exceeding 0.94. It could be seen that after PAV aging and natural aging, the low-temperature performance of asphalt binder is affected by the changes of H_A, H_α, H_β, and H_γ in a similar trend. However, asphalt binder's stiffness modulus under different aging styles showed weak linear correlations with oxygen content, number-average molecular weight, weight-average molecular weight, and polydispersity index, achieving a maximum goodness-of-fit of only 0.62. It could be seen from the figure that the diminished goodness-of-fit primarily stems from the PAV-aged asphalt binder data points significantly deviating the regression curve. This indicated that although laboratory PAV aging had resulted in higher oxygen content, number-average molecular weight, weight-average molecular weight, and polydispersity index of asphalt binder compared to natural aging, the laboratory PAV-aged asphalt binder did not exhibit a greater stiffness modulus. Instead, its stiffness modulus was markedly lower than that of naturally aged asphalt binder. These findings demonstrated that forced aging in the laboratory altered the cross-scale behaviors connecting oxygen content evolution, molecular weight changes, and low-temperature performance variations during asphalt aging.

Although research had established the predominant contribution of thermal-oxidative conditions to the cross-scale behaviors of asphalt binder's macro-micro performance during natural aging, thermal-oxygen-based PAV aging style still failed to restore authentic natural aging behaviors. Future research can achieve more precise aging simulations of asphalt binder by calibrating temperature and oxygen parameters in laboratory aging protocols.

4. Conclusions

In this investigation, comprehensive testing was conducted on asphalt binder's low-temperature performance and microscopic composition across unaged and four distinct aging styles. Macro-micro performance correlations were systematically analyzed, yielding four principal conclusions:

(1) The harsh climate of cold-arid regions accelerated the aging of asphalt binder, with 12-month naturally aged specimens exhibiting significantly inferior low-temperature performance compared to PAV-aged counterparts. It posed a greater challenge to the durability of flexible pavement

(2) Natural aging produced more pronounced changes in four attributed hydrogen content than PAV aging, whereas oxygen content and molecular weight variations were less. The results demonstrated that dehydrogenative condensation and chain scission reactions were not prominently observed during the PAV forced aging process. However, significant oxidation occurred, leading to the formation of more macromolecular structures in the asphalt.

(3) From both macroscopic and microscopic perspectives, thermal-oxidative conditions were identified as the primary cause of asphalt binder aging in natural environments. Environmental factors including light, water, and dust contamination exhibited either accelerating or inhibitory effects on aging processes. The coupling interactions among these multiple factors did not significantly alter the aging progression of asphalt binder.

(4) The PAV-aged asphalt binder data points significantly deviating the regression curve was principally responsible for the poor correlations observed between oxygen content, molecular weight, and low-temperature performance of asphalt binder across different aging styles. This demonstrated that the forced aging of PAV aging fundamentally modified the asphalt binder’s cross-scale behaviors of linking microscopic component composition to macroscopic performance.

Author Contributions: Conceptualization, F.H. and M.G.; methodology, Y.Z.; validation, F.H., M.G. and Y.Z.; formal analysis, B.H.; investigation, B.H.; resources, W.Z.; data curation, F.H.; writing—original draft preparation, F.H.; writing—review and editing, M.G.; visualization, Y.Z.; All authors have read and agreed to the published version of the manuscript.

Funding: This study was supported by National Key R&D Program of China (2024YFB2605102) and National Natural Science Foundation of China (52478429 and U24A20198).

Institutional Review Board Statement: Not applicable.

 doi:10.20944/preprints202509.2463.v1

Informed Consent Statement: Not applicable.

Data Availability Statement: The original contributions presented in the study are included in the article, further inquiries can be directed to the corresponding author.

Conflicts of Interest: The authors declare no conflict of interest.

References

1. Guo M, Yin X, Liang M, et al. Study on effect of thermal, oxidative and ultraviolet coupled aging on rheological properties of asphalt binder and their contribution rates. *International Journal of Pavement Engineering*. 2023, 24(1).
2. Fu C, Wang Z, Song S, et al. Experimental Study on Anti-Aging Effect of Asphalt Binder Liquid Anti-Aging Agent. *Buildings*. 2024, 14(4).
3. Pei Z, Xu M, Cao J, et al. Analysis of the microcharacteristics of different kinds of asphalt based on different aging conditions. *Materials and Structures*. 2022, 55(10).
4. Zhang K, Shen S. Development and Validation of the Coupled Diffusion-Kinetics Aging Model to Analyze Field Aging Gradient in Asphalt Pavements. *Journal of Materials in Civil Engineering*. 2022, 34(8).
5. He Y, Hu Q, Zhao X, et al. Impacts of ultraviolet irradiation on asphalt binder: a comprehensive review. *International Journal of Pavement Engineering*. 2025, 26(1).
6. Yuan J, Li H, Li T, et al. Evolution of asphalt performance under the coupled aging of ultraviolet, high temperature and water. *Case Studies in Construction Materials*. 2024, 20.
7. Guan M, Guo M, Tan Y, et al. Study on the effect of aging on cracking resistance of virgin asphalt binder and its evolution model. *Construction and Building Materials*. 2023, 407.
8. Li Q, Zeng X, Wang J, et al. Aging performance of high viscosity modified asphalt under complex heat-light-water coupled conditions. *Construction and Building Materials*. 2022, 325.
9. Guan M, Guo M, Liu X, et al. Effect of Multifactor Coupling Aging on Rheological Properties of Asphalt Binders and Correlations between Various Rheological Indexes. *Journal of Materials in Civil Engineering*. 2024, 36(5).
10. Traxler R N. Relation between asphalt composition and hardening by volatilization and oxidation. 1961.
11. Liu H, Zhang Z, Tian Z, et al. Exploration for UV Aging Characteristics of Asphalt Binders based on Response Surface Methodology: Insights from the UV Aging Influencing Factors and Their Interactions. *Construction and Building Materials*. 2022, 347.
12. Zhao Y, Wu X, Chao Y, et al. Aging characteristics and microscopic mechanisms of SBS asphalt based on coupled light-heat-water aging. *Construction and Building Materials*. 2024, 456.
13. Hu C, Zhou Z, Luo Y, et al. Effect of Acid Rain on Mechanical Properties and Aging Mechanism of Asphalt. *Journal of Materials in Civil Engineering*. 2023, 35(6).
14. Xing C, Zhu B, Chiang K C K, et al. Effect of Salt Solution Environment on the Aging of Styrene-Butadiene-Styrene (SBS)-Modified Asphalt. *Polymers*. 2024, 16(12).
15. Xu S, Cai S, Huang R, et al. Investigation of aging behaviors of asphalt under the coupling conditions of salt and water. *Fuel*. 2024, 365.
16. Porto M, Caputo P, Loise V, et al. Bitumen and Bitumen Modification: A Review on Latest Advances. *Applied Sciences-Basel*. 2019, 9(4).
17. Wu M, Yin L, Li M, et al. A state-of-the-art review of asphalt aging behavior at macro, micro, and molecular scales. *Construction and Building Materials*. 2025, 460.
18. Siddiqui M N, Ali M F. Investigation of chemical transformations by NMR and GPC during the laboratory aging of Arabian asphalt. *Fuel*. 1999, 78(12): 1407-1416.
19. Ahmad M, Khedmati M, Mensching D, et al. Aging characterization of asphalt binders through multi-aspect analyses: A critical review. *Fuel*. 2024, 376.
20. Zhang S, Hong H, Zhang H, et al. Investigation of anti-aging mechanism of multi-dimensional nanomaterials modified asphalt by FTIR, NMR and GPC. *Construction and Building Materials*. 2021, 305.
21. Di H, Zhang H, Yang E, et al. Usage of Nano-TiO2 or Nano-ZnO in Asphalt to Resist Aging by NMR Spectroscopy and Rheology Technology. *Journal of Materials in Civil Engineering*. 2023, 35(1).

 doi:10.20944/preprints202509.2463.v1

22. Khavandi Khiavi A, Ghanbari A, Ahmadi E. Evaluation of Poly 2-Hydroxyethyl Methacrylate-Modified Bitumen Aging Using NMR and FTIR Techniques. *Journal of Transportation Engineering Part B-Pavements*. 2021, 147(1).
23. Hu D, Gu X, Lyu L, et al. Unraveling oxidative aging behavior of asphaltenes using ab initio molecular dynamics and static density functional theory. *Construction and Building Materials*. 2022, 318.
24. Liu S, Shan L, Li G, et al. Molecular-based asphalt oxidation reaction mechanism and aging resistance optimization strategies based on quantum chemistry. *Materials & Design*. 2022, 223.
25. Wang C, Tian X, Wang Y, et al. The aging mechanism of asphalt aromatics based on density functional theory, Frontier Orbitals, IR, SARA, and GPC. *Journal of Molecular Liquids*. 2024, 396.
26. Liu H, Hao P, Wang H, et al. Effects of Physio-Chemical Factors on Asphalt Aging Behavior. *Journal of Materials in Civil Engineering*. 2014, 26(1): 190-197.
27. Mirwald J, Werkovits S, Camargo I, et al. Investigating bitumen long-term-ageing in the laboratory by spectroscopic analysis of the SARA fractions. *Construction and Building Materials*. 2020, 258.
28. Zou Y, Pang L, Xu S, et al. Investigation of the Rheological Properties and Chemical Structure of Asphalt under Multiple Aging Conditions of Heat, UV and Aqueous Solution. *Materials*. 2022, 15(16).
29. Zhang R, Shi Q, Liu Y, et al. Thermal-oxidative aging characteristics and mechanism of castor seeds oil-based bio-asphalt. *Construction and Building Materials*. 2024, 417.
30. Zhang F, Liu Y, Cao Z, et al. Enhancement of Anti-UV Aging Performance of Asphalt Modified by UV-531/Pigment Violet Composite Light Stabilizers. *Processes*. 2024, 12(12).
31. Wang T, Chen Z, Wang Y, et al. The Effect of Aging on the Molecular Distribution of Crumb Rubber Modified Asphalt Based on the Gel Permeation Chromatography Test. *Buildings*. 2023, 13(5).
32. Guo M, Zhang R, Du X, et al. A State-of-the-Art Review on the Functionality of Ultra-Thin Overlays Towards a Future Low Carbon Road Maintenance. *Engineering*. 2024, 32: 82-98.
33. Crucho J, Picado-Santos L, Neves J, et al. Tecnico accelerated ageing (TEAGE) - a new laboratory approach for bituminous mixture ageing simulation. *International Journal of Pavement Engineering*. 2020, 21(6): 753-765.
34. Yang B, Li H, Sun Y, et al. Chemo-rheological, mechanical, morphology evolution and environmental impact of aged asphalt binder coupling thermal oxidation, ultraviolet radiation and water. *Journal of Cleaner Production.* 2023, 388.
35. Ren S, Liu X, Lin P, et al. Chemo-physical characterization and molecular dynamics simulation of long-term aging behaviors of bitumen. *Construction and Building Materials*. 2021, 302.
36. Ge D, Chen S, You Z, et al. Correlation of DSR Results and FTIR's Carbonyl and Sulfoxide Indexes: Effect of Aging Temperature on Asphalt Rheology. *Journal of Materials in Civil Engineering*. 2019, 31(7).
37. Asif S A, Ahmad N, Asif S U, et al. Effect of Aging on Physical, Chemical, and Thermal Properties of Bitumen. *Journal of Transportation Engineering Part B-Pavements*. 2023, 149(2).
38. Wang S, Huang W, Kang A. Evaluation of Aging Characteristics of High-Viscosity Asphalt: Rheological Properties, Rutting Resistance, Temperature Sensitivity, Homogeneity, and Chemical Composition. *Journal of Materials in Civil Engineering*. 2021, 33(7).
39. Lee S, Amirkhanian S N, Putman B J. Characterization of Recycled Aged RAP Binders Containing Crumb Rubber Modifier Using Gel Permeation Chromatography. *Journal of Materials in Civil Engineering*. 2009, 21(8): 382-391.